ORBITAL AND STORM TIME ANALYSIS OF THE PULSED ELECTROSTATIC TRACTOR

Joseph Hughes and Hanspeter Schaub

Department of Aerospace Engineering, University of Colorado, Boulder, Boulder, USA, Email: {Joseph.Hughes, Hanspeter.Schaub}@colorado.edu

ABSTRACT

The Electrostatic Tractor (ET) is proposed to touchlessly tow tumbling, multi-ton Geosynchronous (GEO) debris objects to a graveyard orbit. The tug craft emits an electron beam onto the debris, charging itself positively and the debris negatively which causes an attractive force. In prior work the beam is continuous, but recent work has suggested pulsing the beam current to slightly increases the force, and opens windows during which measurements can be taken without electrostatic interference. This paper investigates the performance of the pulsed ET subject to normal plasma variations over a orbit, and solar storms. The average pulsed force varies over an orbit, but the optimal balance between current and voltage does not change much. During a storm, the forces are much higher, which would speed the re-orbit time.

Key words: Space Debris, Pulsed Electrostatic Tractor, Space Weather.

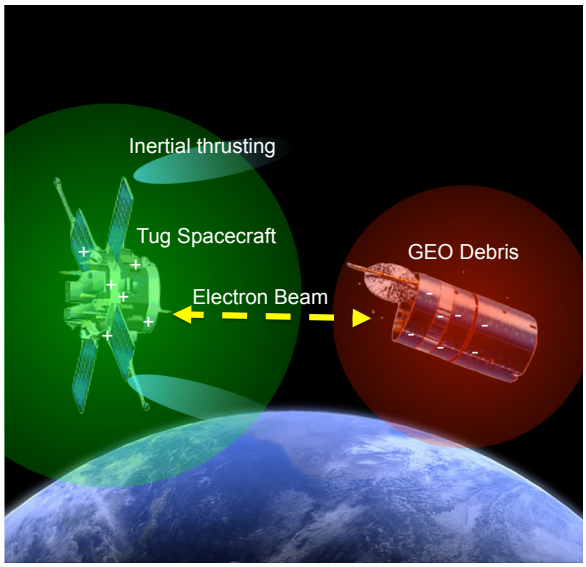

Figure 1. The Electrostatic Tractor (ET) allows spacecraft to touchlessly exert forces and torques on passive space objects

1. INTRODUCTION

The Geosynchronous (GEO) orbit regime is home to at least $18.3 Billion in space assets from the civil, commercial, and defense sectors [6]. Of the 1369 tracked objects in GEO, only 21% are controlled. This crowding of large, often school-bus sized objects creates the probability of collision, which is expected to worsen with current launch and re-orbiting trends [2, 1]. To reduce the collision probability, many concepts have been proposed to move GEO debris into a graveyard orbit about 200 – 250 km above GEO. Some of these require physical contact with the debris object such as harpoons, nets, and robotic arms [24]. These methods are attractive because once contact is made the tug spacecraft can use its thrusters to reorbit the debris object in only a few orbits. The docking process is very challenging and raises strong concerns regarding colliding with the debris and creating more debris. Additionally, the robotic docking solutions discussed in Reference [7] require that the debris be rotating at rates under 1 degree/second. However, many uncontrolled debris objects spin up to many tens of degrees per second [13]. Because of this, methods are needed to de-spin the debris before grappling or touchless tugging solutions are required.

Touchless tugging concepts are more simplistic in that they do not require grappling and are safer in that they reduce the risk of collisions, however, they typically require longer re-orbiting times. The Ion Beam Shepard [5, 14], for example uses a beam of ions to push the debris ahead of the tug. The tug must have an additional thruster that has at least twice the thrust of the ion beam. Another concept is the Electrostatic Tractor (ET) [17, 18], which uses an electron beam to charge a tug spacecraft positive and a debris object negative. An attractive Coulomb force results from this charging. For two moderately sized spacecraft (3m diameter) charged at $\pm$20 kV, and separated by 7 craft radii, the debris feels a 1.2 mN force that could raise its orbit by more than 5 km/day [19]. A tug craft equipped with an electron gun and low thrust motors could move defunct GEO satellites to a graveyard orbit in a matter of months [19]. Additionally, spacecraft with non-symmetric charge distributions will also feel and apply torques through this charging [4, 22, 23]. This torque can be used to touchlessly de-

tumble non-cooperative space objects in a matter of days [3] depending on the debris inertia and spin rate.

A recent consideration to the ET concept is pulsing the electron beam [12]. This gives small force efficiency increases in certain power and voltage regimes, but that analysis is confined to one particular set of plasma parameters for simplicity. In reality, plasma parameters change dramatically over the course of an orbit. Pulsing the beam also provides brief (hundreds of milliseconds) periods where the beam is off and both spacecraft are discharged. This would allow for range measurements, thrusting, and other processes to take place without interference from the electron beam and the highly charged spacecraft. This paper continues this analysis by considering the varying plasma conditions experiences over one orbit, and during a solar storm.

The electron beam is not the only current source that must be accounted for in the ET. The space environment contains free ions and electrons that impact both spacecraft, and the sun frees electrons through the photoelectric effect. The plasma currents depend on the the plasma density and temperature, which depend on local time and the K_p index. The K_p index is a number from 0 to 9 that measures geomagnetic activity which impacts the size and shape of the magnetosphere, and therefore what plasma populations have access to different parts of the GEO orbit. Local time is a measure of the satellite-earth-sun angle; local time is 12:00 at "noon" and 0 or 24 during eclipse.

The GEO space weather can vary drastically even over a nominal 1-day orbit. Denton et. al. discuss in Reference [9] the 10-year averaged GEO space weather conditions. The ET performance is dependent on the local space weather plasma properties [20, 11, 10]. Reference [11] investigate how such nominal and solar storm related space weather conditions impacts the ET performance. The hotter plasma typically requires less beam current to achieve the optimal ET force. However, the performance variations between a nominal beam current and a time-varying optimal current are found to be small with a medium level K_p index. With hotter plasma a nominal beam current might lead to excessive tug charging and no debris charging.

To ascertain the performance impact of plasma variations on the pulsed ET performance, the daily variations at quiet times are first discussed. Next the methods for determining steady-state and average pulsed force are discussed, and a continuous ET is analyzed. The analysis is then expanded to include pulsed beams. Finally, storm conditions are used to analyze continuous and pulsed beams.

2. PROBLEM STATEMENT

The problem of two charged spacecraft with complex geometries interacting electrostaticly in a GEO plasma is a complex one with many independent parameters. In this analysis, the simpler problem of two aluminum spheres is considered. The tug sphere has a radius of $R_T = 2$m, the debris sphere has a radius $R_D = 1.5$m, and the pair are separated by a center to center distance of $\rho = 17$m. A constant pulse period of $T_p = 0.1$ seconds is used.

In this analysis a constant beam power of 16 Watts is considered. For continuous cases, the beam power is simply the beam voltage multiplied by the beam current: $P = I_B V_B$. For a pulsed beam, the average power is attenuated by the duty cycle d since no power is drawn while the beam is off: $P = dI_B V_B$. In order to keep the same power while exploring changes in beam voltage, current, and duty cycle, the following substitutions are used:

$$V_B = \frac{V_{B0}}{\gamma\sqrt{d}} \qquad I_B = \frac{\gamma I_{B0}}{\sqrt{d}} \tag{1}$$

The parameters V_{B0} and I_{B0} are the baseline voltage and current in a continuous beam that have a product of 16 Watts. The factors of $\sqrt{d}$ combine to cancel out the d in the numerator, and γ cancels out of the power equation. The dimensionless tuning parameter γ allows the balance between voltage and current to be varied without changing the power. A γ value greater than 1.0 translates to more current and less voltage than the baseline.

In this analysis, baseline beam voltage and current are given as:

$$V_{B0} = 23.9 \text{ kV} \qquad I_{B0} = 670\ \mu\text{A} \tag{2}$$

These baseline parameters can be used in Eq. (1) to find the actual beam voltage and current given a duty cycle and γ value.

Table 1. Plasma parameter fitting coefficients

	n_e (cm^{-3})	n_i (cm^{-3})	T_e (keV)
a_0	0.9	5	2.3
a_1	0.04804	-0.6345	0.4468
a_2	-0.017	-0.09276	-0.1564
a_3	1.425e-3	0.03558	0.01599
a_4	-5.601e-5	-2.27e-3	-6.948e-4
a_5	9.44e-7	4.144e-5	1.112e-5

The main novel contribution of this paper is expanding the analysis to include daily variations in plasma temperature and densities over an orbit and during a storm. Hogan et. al. [10] used the statistical data provided by Denton et. al. [9] to predict the plasma density and temperature as a function of local time. This model is reused in this analysis. There are two populations of ions at GEO, one hot and tenuous and the other cold and dense. The current delivered by the cold and dense population is much more 20-100 times larger than the hot population, so only the cold population is considered here.

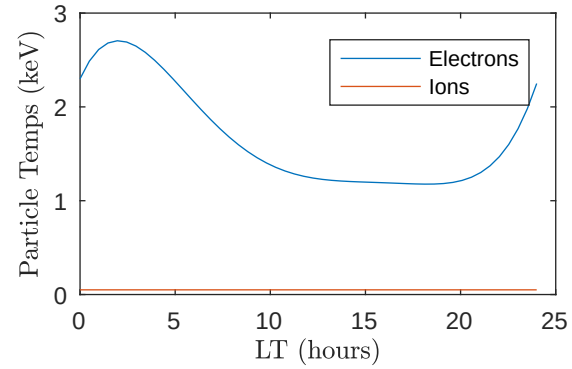

(a) Particle Temperatures

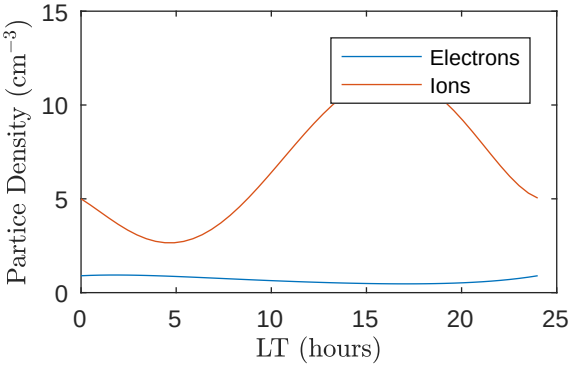

(b) Particle Densities

Figure 2. Plasma density and temperature as a function of local time during quiet ($K_p = 1.5$) conditions

Each parameter (n_e, n_i, T_e, T_i) is predicted from a power series:

$$f(t) = \sum_{i=0}^{5} a_i t^i \tag{3}$$

where t is the local time in hours. This is done for electron and ion densities as well as electron temperature, but as no data is available for ion temperature, a constant value of 50 eV is used. The fitting parameters a_i are given in Table 1. This fit is only valid for the calm space weather condition of $K_p = 1.5$.

The output of these models is shown for the whole local time range in Fig. 2. Keep in mind that only the cold ion population is shown on these plots. During a storm, a K_p index of 8.5 is used and the static parameters $n_e = n_i = 1$ cm^{-3} and $kT_e = kTi = 20$ eV are used. No variation with local time during storm time is considered.

3. METHODS

A numerical simulation is developed to find the currents as a function of both the spacecraft charge levels and time. This is used to propagate the charge on the tug and debris spacecraft $[q_\mathrm{T}, q_\mathrm{D}]^T$ through time. This is shown explicitly below:

$$\begin{bmatrix} \dot{q}_\mathrm{T} \\ \dot{q}_\mathrm{D} \end{bmatrix} = \begin{bmatrix} \sum I_\mathrm{T}(q_\mathrm{T}, q_\mathrm{D}, t) \\ \sum I_\mathrm{D}(q_\mathrm{T}, q_\mathrm{D}, t) \end{bmatrix} \tag{4}$$

Here, q_D and q_T are the charges of the debris and tug spacecraft, and I_D and I_T are the currents on the debris and tug spacecraft. The beam is a time-varying current when it is pulsed. The currents on each spacecraft are functions of the voltage of each, which are determined by the charges. A mapping between charges and voltages is given by the elastance matrix [21, 22] as:

$$\begin{bmatrix} \phi_\mathrm{T} \\ \phi_\mathrm{D} \end{bmatrix} = \frac{1}{4\pi\epsilon_0} \begin{bmatrix} 1/R_\mathrm{T} & 1/\rho \\ 1/\rho & 1/R_\mathrm{D} \end{bmatrix} \begin{bmatrix} q_\mathrm{T} \\ q_\mathrm{D} \end{bmatrix} \tag{5}$$

where ϕ_T and ϕ_D are the voltages, q_T and q_D are the charges, R_T and R_D are the craft radii, and ρ is the center-to-center separation for the tug and debris respectively.

All of the currents are discussed in greater detail in the Appendix. The charging model includes plasma charge flux onto the spacecraft, electron backscattering, electron and ion induced secondary electron emissions, the tug's electron beam itself, as well as the photo electron currents. The models used for Secondary Electron Emission (SEE) via incident electrons, electron backscattering, and SEE via incident ions are those proposed by Lin and Joy [16] and the Nascap Scientific Documentation [8], respectively. Experimental values for the SEE material parameters can vary by more than a factor of 6 [16], which adds uncertainty to charging. Further analysis is needed to investigate the robustness of these findings to variability in SEE model parameters. the cessation of the photoelectric current during eclipse is not included, as it only happens very infrequently at equinoxes.

This forced ordinary differential equation is solved numerically for the charges at each instant using Matlab's built-in integrator, ODE45. This is run with an absolute tolerance of 10^{-9} corresponding to 1 nC, and a relative tolerance of 10^{-3} corresponding to about 3 significant figures. The force at each instant is given by

$$F = \frac{q_T q_D}{4\pi\epsilon_0 \rho^2} \tag{6}$$

where ρ is the center-to-center separation of the spacecraft, and sheath shielding has been neglected. The timespan of integration is 0.2 seconds for the continuous cases, and 3 pulse periods for the pulsed cases. The charge, voltage, and force history are computed for an example pulsed and continuous case with $V_B = 23.9$ kV and $I_B = 536\mu$A for the continuous case, and $d = 0.5, V_B = 42.25$ kV, and $I_B = 758\mu$A for the pulsed case. Both of these sets have an average power of 16 Watts. This simulation talks place at a local time of 10 hours. The output is shown in Fig. 3

The voltage, charge, and force history are shown for pulsed and continuous cases. The continuous cases have

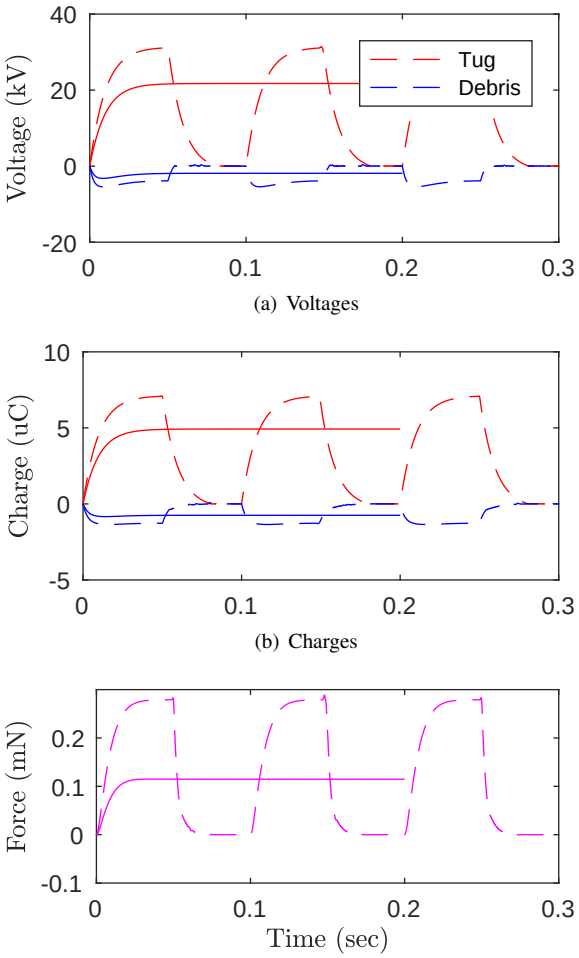

(a) Voltages

(b) Charges

(c) Force

Figure 3. Voltage, charges, and force for pulsed and continuous beams. The tug is red, the debris blue, and pulsed beams are dashed lines while continuous beams are continuous lines

continuous lines while the pulsed have dashed lines. The tug is red and the debris is blue in all the voltage and charge plots. When the beam is on, the pulsed voltage, charges, and force are all higher than the continuous beam, but once the beam turns off all of these decay to zero.

Since the force is proportional to the product of the charges, its increase during the time the beam is on outweighs the decrease in the average force during the time the beam is off. In this example, at this local time, the continuous force is 0.114 mN and the average pulsed force is 0.123 mN, an 8% force increase. The force at the final time step is stored for continuous cases, and the average force is stored for pulsed cases.

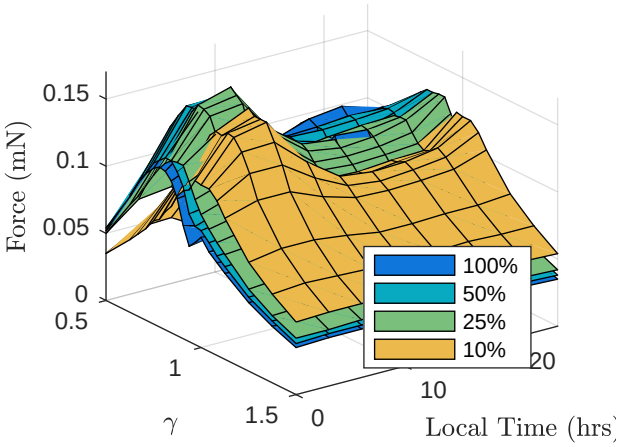

Figure 4. Force as a function of local time, γ, and duty cycle

4. ORBITAL VARIATIONS FOR THE PULSED ELECTROSTATIC TRACTOR

The simulation is run at 9 values of local time between 0 and 24 hours for many values of γ and 4 values for the duty cycle: 10%, 25%, 50%, and the continuous case – 100%. The results are recorded in a large text file and plotted below in Fig. 4. The average or steady-state force is plotted against the local time and γ, with different color surfaces showing different duty cycles.

Each separate duty cycle has a peak in force at a different γ value, with the lower duty cycle beams perform better with higher γ values, meaning more current than voltage. Additionally, the best γ varies slightly over an orbit, but the change in γ and the force increase from varying γ is small. Because of this, there is little benefit to varying the beam voltage or current during an orbit.

The $d = 50\%$ and 25% beams hold the top position at different local times. The maximum pulsed force of 0.168 mN occurs at $LT = 6$, with a 25% duty cycle and $\gamma = 0.8119$. This is 12% higher than the maximum continuous force of 0.15 mN.

During the orbit, the force peaks at a local time of 5 which corresponds to high electron temperatures and low ion density. These two things help the debris to charge very negative, which will increase the force. The fundamental reason for high energy electrons and low ion density in the early morning are that electrons injected at the eclipse point from magnetic reconnection drift counter clockwise around earth while ions drift clockwise. This enriches the early morning sector with high energy electrons. In the afternoon the forces are mostly flat, which suggests that the electron temperature (which also is flat) is a bigger driver than the ion density.

To find the beam parameters that give the most force at this power level, the forces are averaged across an or-

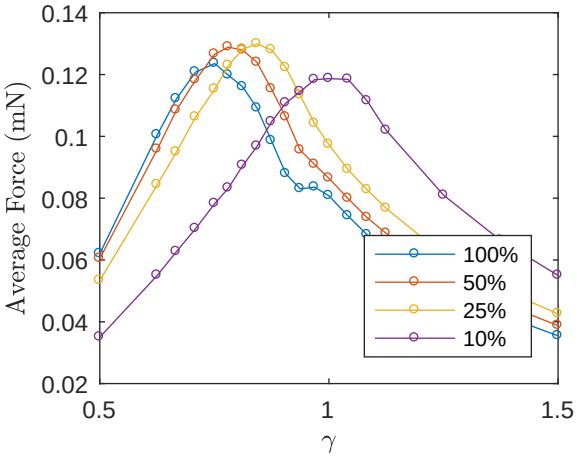

Figure 5. Orbit-averaged force for various γ and duty cycles

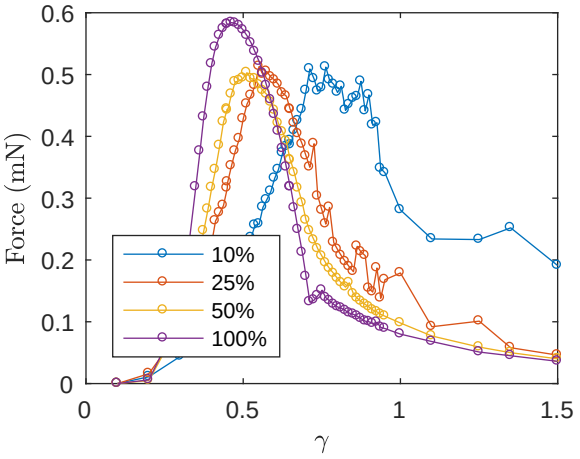

Figure 6. Electrostatc force as a function of duty cycle and tuning parameter γ during a solar storm

bit. This corresponds to averaging each of the sheets in Fig. 4 across local time. This orbit-averaged force is the most applicable to predict orbit raising performance and is shown in Fig. 5

The highest orbit-averaged force of 0.1299 mN occurs with a duty cycle of 25% and $\gamma = 0.8433$. This force is 5.1% higher than the highest continuous force (100% duty cycle) of 0.1236 mN. Considering a 2 month long tow period to the graveyard orbit, this translates to a 3 day savings. In addition to having slightly higher force, pulsing the beam opens up 75 ms windows where both craft are discharged and measurements can be taken without interference from the beam or the charged spacecraft.

5. STORM TIME ANALYSIS OF THE PULSED ET

In the quiet conditions of $Kp = 1.5$, the pulsed tractor has very slight (5.1%) force increases over the continuous beam, and also opens up windows. Of interest is if this performance continues during a solar storm. Solar storms occur when the sun emits a Coronal Mass Ejection (CME) or solar flare which compresses earth's magnetosphere and causes large scale changes in the plasma environment. In this analysis a constant plasma with $n_e = n_i = 1$ cm^{-3} and $kT_e = kT_i = 20$ keV is assumed. Duty cycle and γ are varied to find the highest forces for pulsed and continuous beams. The average forces are shown in Fig. 6

Similar to quiet analysis, there is a maximum force found by varying γ at each duty cycle. However, that best γ is much lower (near 0.5, rather than 0.84) than for quiet solar conditions, which translates to a higher voltage and lower current. The forces are also much higher – the maximum continuous force is 0.584 mN, almost 5 times stronger than the maximum continuous force during quiet solar conditions.

The drop off in force from using a non-optimal γ is much steeper during a storm. This narrower peak means that setting the correct γ becomes more important to achieve the highest force. Additionally, the 10% duty cycle looks much different from all others during a storm and lacks a smooth peak. The trend found in quiet conditions of lower duty cycles requiring higher γ values is preserved. In storm conditions, the continuous beam produces more force, but the strongest pulsed beam is only 14% weaker and opens large windows of opportunity.

The reason the force is so much higher during the storm is that while normally the two spacecraft can only differ by the accelerating voltage of the electron beam, during a storm the plasma itself contributes to the charging. For a 40 keV electron beam used in quiet solar conditions, the tug can only be 40 kV higher in voltage than debris, because once they are more than 40 kV apart, the beam will not be able to reach the debris but rather deflect and never return, or circle back and impact the tug. This will cause a steady-state scenario with voltages around $V_T = 30$ kV and $V_D = -10$ kV depending on the relative sizes of the tug and debris. During a storm, the tug may charge to the voltage of the beam (40 keV in this example) while the debris is charged not by the beam but rather by the plasma electrons to roughly their temperature, 20 keV. This will result in a steady state scenario with $V_T = 40$ keV and $V_D = -20$ keV. The larger voltages allow for much more charge, which leads to the much higher forces.

Solar storms increase the force and change the beam parameters that product the highest force. However, using the best case for quiet solar conditions ($d = 0.25, \gamma = 0.8433$) gives a force increase to 0.189 from 0.1299 mN. Solar storms are infrequent, and only last for around 3 days, with peak conditions being observed for even shorter times. Solar activity above $K_p = 7$ is only observed 1.5% of the time [9], so it is doubtful that these conditions would be experienced on a single debris tow. However, if they were, they would shorten the mission

through the increased force.

6. CONCLUSIONS

This paper analyzes the force produced by the pulsed electrostatic tractor during an orbit in low solar storm conditions, and during a storm. For the quiet solar condition analysis, the best duty cycle and γ value do not change much, and switching to the best one at that local time does not cause large force increases. This suggests that a design team could opt for a constant beam voltage, current, and duty cycle to simplify the mission and not give up much in performance.

During a storm, the forces at nearly all duty cycles and γ values increase due to the high electron and ion temperatures. The optimal balance between current and voltage shifts to favor a higher voltage beam, however, if the best value for non-storm conditions is used, the force still doubles. During storm times, continuous beams perform better than pulsed ones. Since high storm conditions are infrequent, they will not likely be encountered in a mission, but if they do they will speed the towing of the debris to a graveyard orbit.

Overall, adding local time variations and storm analysis does not greatly change the pulsed electrostatic tractor. In some cases it produces more force at the same power level, and in all situations it opens large windows during which both craft are discharged and can take measurements without interference from the beam.

7. APPENDIX – CHARGING MODEL

Both spacecraft are subject to many environmental currents as well as a pulsed electron beam. The environmental currents are a function of the space plasma parameters and the voltage of the spacecraft (ϕ), and the electron beam is a function of time. The change in charge with time is the sum of the currents, which yields a forced ordinary differential equation for the charge on a spacecraft.

$$\frac{\mathrm{d}q}{\mathrm{d}t} = I_{\text{beam}}(t)(1 - Y_B(E_L)) + I_{\text{e}}(\phi)(1 - < Y_e > (\phi)) + I_{\text{i}}(\phi)(1 + < Y_i > (\phi)) + I_{\text{p}}(\phi) \tag{7}$$

Where the environmental currents considered are the electron and ion plasma current (I_e and I_i), and the photoelectric current (I_p). Electron currents (plasma and beam) are attenuated by SEE and backscattering, while the ion plasma current is increased by SEE. These effects are combined in the yields for the beam, electron current, and ion current ($Y_B, Y_e,$ and Y_i). Each of these currents are described individually. The electron beam is typically chosen to be much larger than any other currents.

7.1. Electron Plasma Current

Electrons at GEO are tenuous and hot. The orbit motion limited (OML) method given by [15] is used to calculate the electron current.

$$I_{\text{e}} = \begin{cases} -\frac{Aqn_e v_{\text{th}_{\text{e}}}}{4} e^{q\phi/k_{\text{B}}T_{\text{e}}} & \phi < 0 \quad (8) \\ -\frac{Aqn_{\text{e}} v_{\text{th}_{\text{e}}}}{4}(1 - \frac{q\phi}{k_{\text{B}}T_{\text{e}}}) & \phi \geq 0 \quad (9) \end{cases}$$

Where I_{e} is the electron plasma current [A], A is the spacecraft area [m^2], q is the fundamental charge [C], n_{e} is the electron density [#/m^3], $v_{\text{th}_{\text{e}}}$ is the electron thermal speed [m/s], which is given for either species by $v_{\text{th}} = \sqrt{2k_{\text{B}}T/\pi m}$. The spacecraft voltage is ϕ [V], and $k_{\text{B}}T_{\text{e}}$ is the electron thermal energy [eV].

7.1.1. Electron-Induced SEE and Backscattering

When an electron impacts a material it can impart some of its energy to the surrounding electrons, which may be ejected. These ejected electrons typically have very low energies ($\sim$2 eV) but can cause a net current for a negative craft. The probability of a secondary electron being ejected is dependent on the landing energy of the incident electron and the angle of incidence. In this analysis only normal incidence is considered. The dimensionless ratio of incoming incident electrons to outgoing secondary electrons as a function of landing energy is given by Lin and Joy [16]:

$$\delta(E) = \delta_M 1.28\left(\frac{E}{E_{\text{Me}}}\right)^{-0.67}(1 - e^{-1.614(\frac{E}{E_{\text{Me}}})^{1.67}}) \tag{10}$$

Backscattering occurs when an electron is reflected from the spacecraft rather than absorbed. This analysis uses the model provided by the Nascap Scientific Documentation for energy-dependent backscattering [8]:

$$\eta(E) = \left(\frac{H(1-E)H(E-0.05)\log(\frac{E}{0.05})}{\log(20)} + H(E-1)\right) \times (\frac{e^{-E/5}}{10} + 1 - (2/e)^{0.037Z}) \tag{11}$$

Where η is the dimensionless probability of backscattering, E is the landing energy in keV, $H(x)$ is the heaviside step function, and Z is the atomic number of the material (aluminum in this analysis). The formulas above can be added to produce the total yield $Y(E) = \eta(E) + \delta(E)$ for incident monoenergitic electrons.

7.2. Ion Plasma Current

The ion plasma current is a result of the ions impacting the spacecraft, absorbing an electron, and leaving the system. The model is similar to the electron plasma current

with a polarity flip [15].

$$I_i = \begin{cases} -\frac{Aqn_{\mathrm{i}}v_{\mathrm{th_i}}}{4} e^{q\phi/k_{\mathrm{B}}T_{\mathrm{i}}} & \phi > 0 \quad (12) \\ -\frac{Aqn_{\mathrm{i}}v_{\mathrm{th_i}}}{4}\left(1 - \frac{q\phi}{k_{\mathrm{B}}T_{\mathrm{i}}}\right) & \phi \leq 0 \quad (13) \end{cases}$$

Where $v_{\mathrm{th_i}}$ and $k_{\mathrm{B}}T_{\mathrm{i}}$ are the ion thermal speed [m/s] and thermal energy [eV], respectively. All ions are assumed to be protons. For both ions and electrons, the current absorbed from the attracted species at high potentials is approximately linear, and the current from the repulsed species exponentially decays with voltage.

7.3. Ion-induced SEE

Ions may also cause SEE, and for many materials the number of secondaries caused by ions is much larger than that caused by electrons. However, since the ion current is usually much smaller than the electron current, ion-induced SEE is neglected in many cases. For this application, where the spacecraft voltage exceeds the plasma temperature by an order of magnitude, ion-induced SEE must be considered.

In this analysis the two parameter Nascap model [8] is used:

$$\delta(E) = \frac{\beta E^{1/2}}{1 + E/E_M} \quad (14)$$

7.4. Total Yields

If the space plasma were monoenergetic, Eqns. (10), (11) and (14) would be enough to form the total yields $\langle Y_e \rangle$ and $\langle Y_i \rangle$. However, space plasma is not monoenergetic, and in this analysis a Maxwellian flux distribution is used.

$$F(E) \propto Ee^{-E/kT_e} \quad (15)$$

The mean yield is found by integrating the product of the total yield and the current with respect to energy, and normalizing by the total current:

$$\langle Y \rangle = \frac{\int_L^\infty Y(E)\, E \exp(-\frac{E \pm V}{kT}) dE}{\int_L^\infty E \exp(-\frac{E \pm V}{kT}) dE} \quad (16)$$

For the $\pm$ and $\mp$ terms, the top sign is for the ions while the lower sign is for electrons. This integral is solved numerically using the u substitution $u = \exp(-(E \pm V)/kT)$ for the attracted species and $u = \exp(-E/kT)$ for the repulsed species. This transforms the integration domain from $E \in [L, \infty]$ to $u \in [0, 1]$. This is solved numerically using an iterative Gauss-Legendre quadrature based integrator. This solver is chosen over simpler numeric integration schemes like Simpson's Rule or the Trapezoidal method because it allows the user to specify the error tolerance. For this application, an error tolerance of 10^{-6} is used.

These yields are interpolated rather than calculated at each timestep for time savings. The yields are a function of the spacecraft voltage, and the particle temperature. The variations in particle temperature shown in Fig. 2(a) are used to determine the particle temperatures as a function of local time. Additionally, the spacecraft voltage is varied from -100 kV to 100 kV to make a large dataset of yields for electrons and ions. At each timestep, the local time and spacecraft are used to interpolate the yields from the dataset. The yields as a function of local time and spacecraft voltage are shown in Fig. 7.

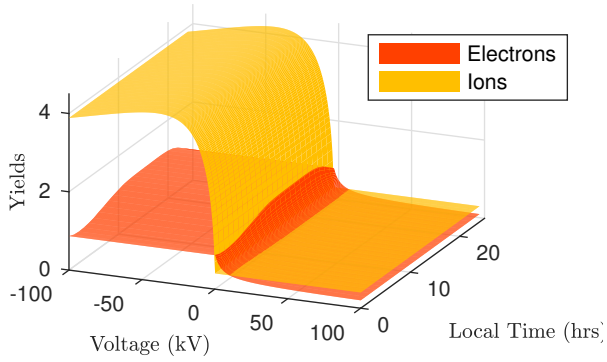

Figure 7. Electron and ion-induced yields as a function of local time and spacecraft voltage for low K_p

Since the ion temperature is constant, the ion-induced SEE is not a function of local time. Since there is only a voltage dependency for the attracted species, the yield is only a function of local time for the repulsed species. The ion yield is much larger than the electron yield, but due to the electron's higher mobility the electron induced SEE make a larger difference.

For the storm-time analysis, the constant temperatures of $kT_e = kT_i = 20$ keV are used. Curves rather than surfaces are used to interpolate the electrona nd ion yields as a function of spacecraft voltage.

7.5. Photoelectron Current

Energy from the sun can energize electrons in the first few nanometers of the spacecraft surface so that they leave the surface. The fraction that have enough energy to escape the potential well of the spacecraft cause a net positive current given by [15]:

$$I_p = \begin{cases} j_{\mathrm{ph}} A_l e^{-q\phi/k_{\mathrm{B}}T_{\mathrm{ph}}} & \phi > 0 \quad (17) \\ j_{\mathrm{ph}} A_l & \phi \leq 0 \quad (18) \end{cases}$$

Where j_{ph} is the photoelectron flux [A/m^2], A_l is the illuminated area [m^2], and $k_{\mathrm{B}}T_{ph}$ is the thermal energy of the ejected photoelectrons [eV]. For a negative spacecraft this current is constant, and for a positively charged spacecraft it quickly vanishes.

7.5.1. Electron Beam

If a beam of electrons is shot from the tug craft to the deputy craft, it will cause a positive current on the tug and a negative current on the deputy. If the beam does not have sufficient energy to escape the potential well of the tug, it will return and cause no net currents. If it has sufficient energy to leave the well of the tug, but insufficient energy to reach the deputy, the beam will diverge and disperse. These electrons have sufficient energy to escape the system, but some may impact the tug before they have a chance to escape. Further analysis is needed to quantify the fraction that do not escape, but in this analysis it is assumed to be negligible. This is a good assumption considering spacecraft with complex geometries and separation larger than radii. The currents on the debris are then given by:

$$I_{\text{bd}} = \begin{cases} -I_{\text{b}} & V_{\text{b}} > \phi_{\text{T}} - \phi_{\text{D}} \quad (19) \\ 0 & V_{\text{b}} < \phi_{\text{T}} - \phi_{\text{D}} \quad (20) \end{cases}$$

Where I_{bd} is the beam current on the deputy [A], V_b is the accelerating voltage of the beam [V], and ϕ_t and ϕ_d are the potentials of the tug and deputy spacecraft, respectively. The currents on the tug are given by:

$$I_{\text{bt}} = \begin{cases} I_{\text{b}} & V_{\text{b}} > \phi_{\text{T}} \quad (21) \\ 0 & V_{\text{b}} < \phi_{\text{T}} - \phi_{\text{D}} \quad (22) \end{cases}$$

7.5.2. Beam-Induced SEE

Since the beam is monoenergetic, the mean yield does not need to be computed. The landing energy is computed as

$$E_L = |q_e|(V_B - V_T + V_D) \quad (23)$$

and the SEE and backscattering coefficients can be evaluated directly as

$$Y_B(E_L) = \eta(E_L) + \delta(E_L) \quad (24)$$

without integrating over the flux distribution.

REFERENCES

1. Anderson, P. V. & Schaub, H. 2013, Advances in Space Research, 51, 2195
2. Anderson, P. V. & Schaub, H. 2014, Acta Astronautica, 94, 619
3. Bennett, T. & Schaub, H. 2014, in AAS/AIAA Spaceflight Mechanics Meeting
4. Bennett, T., Stevenson, D., Hogan, E., McManus, L., & Schaub, H. 2014, in 3rd European Workshop on Space Debris Modeling and Remediation, CNES, Paris
5. Bombardelli, C. & Pelaez, J. 2011, AIAA Journal of Guidance, Control, and Dynamics, 34, 916
6. Chrystal, P., McKnight, D., Meredith, P. L., et al. 2011, Space Debris: On Collision Course for Insurers?, Tech. Rep. 1504360-11-en, Swiss Reinsurance Company Ltd, Zürich, Switzerland
7. Couzin, P., Teti, F., & Rembala, R. 2012, in 2nd European Workshop on Active Debris Removal, Paris, France, paper #7.5
8. Davis, V. & Mandell, M. J. 2011, Plasma Interactions with Spacecraft. Volume 2, NASCAP-2K Scientific Documentation for Version 4.1, 4th edn., Science Applications International Corp
9. Denton, M. H., Thomsen, M. F., Korth, H., et al. 2005, Journal of Geophysical Research, 110
10. Hogan, E. & Schaub, H. 2016, Journal of Astronautical Sciences, 63, 237
11. Hogan, E. A. & Schaub, H. 2014, IEEE Transactions on Plasma Science, 43, 3115
12. Hughes, J. & Schaub, H. 2017, IEEE Transactions on Plasma Science
13. Karavaev, Y. S., Kopyatkevich, R. M., Mishina, M. N., et al. 2004, Advances in the Astronautical Sciences, 119
14. Kitamura, S. 2010, in 61st International Astronautical Congress, Prague, Czech Republic
15. Lai, S. T. 2011, Fundamentals of Spacecraft Charging: Spacecraft Interactions with Space Plasmas (Princeton University Press)
16. Lin, Y. & Joy, D. C. 2005, Surface and Interface Analysis, 57, 895
17. Moorer, D. F. & Schaub, H. 2011, Electrostatic Spacecraft Reorbiter, US Patent 8,205,838 B2
18. Schaub, H. & Moorer, D. F. 2014, The Journal of the Astronautical Sciences, 59, 161
19. Schaub, H. & Sternovsky, Z. 2013, in 6th European Conference on Space Debris, ESOC, Darmstadt, Germany, paper No. 6b.O-5
20. Schaub, H. & Sternovsky, Z. 2013, Advances in Space Research, 53, 110
21. Smythe, W. R. 1968, Static and Dynamic Electricity, 3rd edn. (McGraw–Hill)
22. Stevenson, D. & Schaub, H. 2013, Advances in Space Research, 51, 10
23. Stevenson, D. & Schaub, H. 2013, in 5th International Conference on Spacecraft Formation Flying Missions and Technologies, Münich, Germany
24. Wormnes, K., Le Letty, R., Summerer, L., et al. 2013, in Proceedings of the 6th IAASS Conference: Safety is Not an Option, 3–4